Electromagnetic response of a point-dipole crystal

K. Kempa,* R. Ruppin,† and J. B. Pendry
Condensed Matter Theory Group, The Blackett Laboratory, Imperial College, London SW7 2BZ, UK
(Received 7 August 2005; published 2 November 2005)

We study the electromagnetic response of a cubic array of polarizable and resonant point dipoles. We show, that in addition to the formation of photonic and polaritonic bands and gaps in the dispersion of transverse waves, the array allows for bulk and surface plasmon wave propagation, as well as negative refraction in a polaritonic band, and subwavelength lensing. We suggest experimental arrangements for demonstration of these effects, both at microwave and optical frequencies.

DOI: 10.1103/PhysRevB.72.205103 PACS number(s): 78.20.−e, 42.70.Qs, 42.25.Gy, 73.20.Mf

In an early attempt to model the electromagnetic response of an atomic crystal, Mahan and Obermair (MO) developed a theory for electromagnetic wave propagation in an array of point dipoles, and developed a simple, exact formula for the band structure of the transverses modes.[1] Their theory, however, has not been applicable to atomic crystals, because the wave function overlap between the neighboring atoms in such a crystal renders invalid the separability of the electronic and photonic degrees of freedom, implied explicitly in the point dipole model. On the other hand, the point dipole model and MO theory have been shown to properly describe the electromagnetic response of quantum dots.[2] In such a system, nanoscopic islands of electrons (quantum dots), generated at semiconductor interfaces either by doping or an electrode arrangement, had dimensions much smaller than the wavelength of the electromagnetic radiation, i.e., $D \ll \lambda$, and the inter-dot separation was big enough to avoid the wave function overlap. Thus, the conditions for applicability of the point dipole model were satisfied. At present, periodic arrays of point dipoles (point dipole crystals) can be fabricated by a variety of techniques, and thus the MO theory, which describes them very well acquired a new importance. In this paper, we use this theory to study in detail the electromagnetic response of a cubic point dipole array. We show, that in addition to the formation of photonic and polaritonic bands and gaps in the dispersion of transverse waves, the array allows for bulk and surface plasmon wave propagation, as well as negative refraction in a polaritonic band, and subwavelength lensing. We also suggest experimental arrangements for demonstration of these effects, both at microwave and optical frequencies.

According to MO theory the fully retarded dispersion of a transverse electromagnetic (TEM) wave propagating through a point dipole crystal is given by[1]

$$1 = 4\pi\alpha\left(\frac{1}{2}\frac{\Omega \sin\Omega}{\cos\Omega - \cos(n\Omega)} - T_T(k)\right) \tag{1}$$

where

$$n\Omega = ka = K \tag{2}$$

$$\Omega = \omega a/c \tag{3}$$

α is the polarizability per unit volume of the crystal, ω is the frequency, k is the wave vector, c speed of light, a is the lattice constant, and n is the refractive index. Assuming that the crystal is simple cubic, with the lattice vector $\vec{R} = (i,j,m)a$ (i,j,m integers), and that the charge displacements are along [100] or equivalent directions, it can be shown that

$$T(K) = \frac{1}{4\pi}\sum_{i=-I}^{I}\sum_{j=-I}^{I}\sum_{m=-M}^{M}\frac{\cos(Kp)}{(i^2+j^2+m^2)^{3/2}}\left[1 - \frac{3m^2}{i^2+j^2+m^2}\right] \tag{4}$$

where I and $M \to \infty$. For the *transverse* charge displacements $T(K) = T_T(K)$ and $p = i$, (or $p = j$). For the *longitudinal* charge displacements $T(K) = T_L(K)$ and $p = m$.

In the long wavelength ($a \ll \lambda/2\pi$), or equivalently in the nonretarded ($c \to \infty$) limits, $\Omega \ll 1$, and then Eq. (1) becomes

$$n^2 = \varepsilon(\Omega, K) = 1 + 4\pi\alpha/[1 + 4\pi\alpha T_T(K)] \tag{5}$$

where $\varepsilon(\Omega, K)$ is the transverse dielectric function. According to Eq. (5), the polarization of the crystal is given by $\alpha E/[1 + 4\pi\alpha T_T(K)]$ and, therefore, it becomes singular for

$$1 + 4\pi\alpha T_T(K) = 0 \tag{6}$$

At this condition, polarization can be finite even for a vanishing applied electric field E, and thus Eq. (6) is the condition for the transverse *polarization* (TP) *eigenmode* of the crystal. The fully retarded treatment used in Ref. 1, conducted in the Coulomb gauge shows that the general condition for the *longitudinal* (LP) *eigenmode* has also the form of Eq. (6), but with the transverse $T_T(K)$ replaced by the longitudinal $T_L(K)$.

The sums in Eq. (4) can be easily evaluated numerically, since only one of them is slowly convergent. This is the sum along the lines of dipoles with induced charge displacements along the lines, i.e., the m-summation in Eq. (4). It requires, in general, more than a few hundred terms to provide better than 0.1% convergency. The remaining sums (i and j) are rapidly convergent. The main difference between the transverse and longitudinal case is the fact that while for the *transverse* case we can use the following approximation

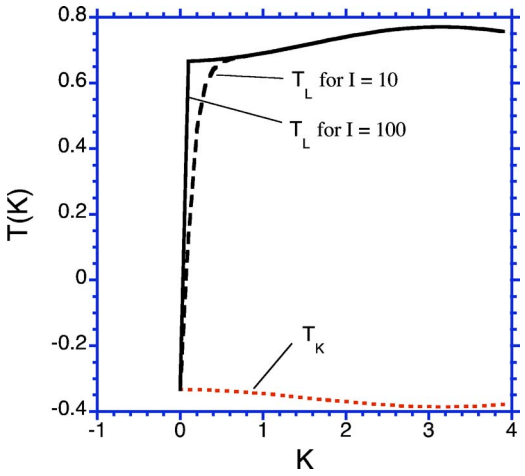

FIG. 1. (Color online) $T(K)$ vs K, for varying summation ranges I and M.

$$T_T(K) \approx v(0) + 2v(1)\cos(K), \tag{7a}$$

where

$$v(i) = \frac{1}{4\pi}\sum_{j=-\infty}^{\infty}\sum_{m=-\infty}^{\infty}\frac{1}{(i^2+j^2+m^2)^{3/2}}\left[1-\frac{3m^2}{i^2+j^2+m^2}\right] \tag{7b}$$

$$v(0) = -0.3594 \quad v(1) = 0.013\,03 \tag{7c}$$

for the *longitudinal* case, in general, a large number of cosine terms contributes to the sum in Eq. (4).

Figure 1 illustrates the behavior of $T(K)$, for varying summation ranges I and M. For $K=0$

$$T_L(0) = T_T(0) = -\tfrac{1}{3} \tag{8}$$

which is required by the Lorentz-correction argument. For larger K there is a region in which $T_L(K)$ progresses rapidly from the $-1/3$ value at $K=0$ to a simple cosine form

$$T_L(K) \approx 0.719\,29 - 0.052\,63\cos(K) \tag{9}$$

"Sharpness" of this transition increases with the number of the dipole rows included in the summation, i.e., with increasing I. This progression is clearly visible in Fig. 1, which shows a very sharp transition already for $I=100$. Eventually, for $I\to\infty$ a step function is obtained, with the discontinuity at $K=0$. This is a very well known, cross-dimensional behavior of polarization modes, similar to that in metallic superlattices,[3] multiwall carbon nanotubes,[4] or single-wall nanotube bundles.[5] While in a single metallic layer (or a single-wall nanotube) there are gapless plasmons, in the infinite superlattice of the metallic planes (and multiwall nanotube, or a infinite bundle of single-wall nanotubes) a gap must open in the plasmon spectrum reflecting the three-dimensional (3D) behavior of the systems. The same effect occurs here. With increasing I, which measures the size of the dipole-line "bundle," the gap develops for $K \gg 1/I$. Fig. 1 also shows that

$$T_L(0^+) - T_T(0) = 1 \tag{10}$$

Using the calculated $T(K)$, the dispersions for the polarization eigenmodes can be obtained from Eq. (6). Assuming simple, harmonic oscillations of the induced polarization charges for a single dipole, we get

$$\alpha(\omega) = \frac{\omega_p^2}{4\pi(\omega_0^2-\omega^2)} = \frac{\Omega_p^2}{4\pi(\Omega_0^2-\Omega^2)} \tag{11}$$

where $\Omega_0=\omega_0 a/c$, $\Omega_p=\omega_p a/c$, ω_0 is the resonance frequency of the charges, and ω_p is a constant, with dimensions of a frequency.

The form of $\alpha(\omega)$ given by Eq. (11) is quite general. It is valid, for example, for metallic systems such as nanoparticles, in which case ω_0 is the well known Mie resonance,[6] and for quantum dots.[2] It was shown[2] that as long as the potential confining electrons inside a metallic unit is parabolic ($m\omega_0^2x^2/2$), its resonant absorption is at frequency ω_0, i.e., each dot responds to radiation as a simple harmonic oscillator, and electron-electron interactions do not affect the response. In this case also $\omega_p^2=4\pi Ne^2/Vm^*$ is the reduced plasma frequency of the electrons, with N the total number of electrons in the entire system, V the total volume of the entire system, m^* the effective electron mass, and e the electron charge.

Using Eq. (11) we obtain from Eq. (6)

$$\Omega = \Omega_i(K) = \sqrt{\Omega_0^2 + \Omega_p^2 T_i(K)} \tag{12}$$

where $i=T$ for the TP, and $i=L$ for the LP mode. While the LP mode, with the dispersion given by Eq. (12), is a legitimate eigenmode in the presence of the photon field, the TP eigenmode given by Eq. (12), is not. Instead, the interaction with photons simply renormalizes the nonretarded transverse polarization charge oscillations yielding the TEM polariton mode given by Eq. (1). On the other hand, the fully retarded treatment leading to Eq. (1), conducted in the Coulomb gauge,[1,7] shows that the longitudinal propagating modes in the crystal are electromagnetically nonretarded,[8] i.e., they do not couple to the photon field in the limit of an infinite crystal. The coupling can be achieved by breaking the perfect translational invariance of the crystal, e.g., by introducing a surface.

The TEM polariton dispersion from Eq. (1), in the long-wavelength limit ($\Omega \ll 1$) is given by

$$\Omega = \sqrt{\frac{\bar{\Omega}_L^2(K)+K^2}{2} \pm \sqrt{\left(\frac{\bar{\Omega}_L^2(K)+K^2}{2}\right)^2 - K^2\Omega_T^2(K)}} \tag{13}$$

where

$$\bar{\Omega}_L(K) = \sqrt{\Omega_T^2(K)+\Omega_p^2} \tag{14}$$

The corresponding mode structure is shown in Fig. 2, for $\Omega_0=\Omega_p=0.2$. Solid lines represent the TEM branches as given by Eq. (13). The upper dot-dashed line is for the LP, and the lower dashed for the TP mode. Inset in the upper-left corner shows a zoomed-in section of the dispersion diagram with clearly visible parabolic dispersions of both, the TEM upper branch, and the LP mode. The asymptotics of the TEM

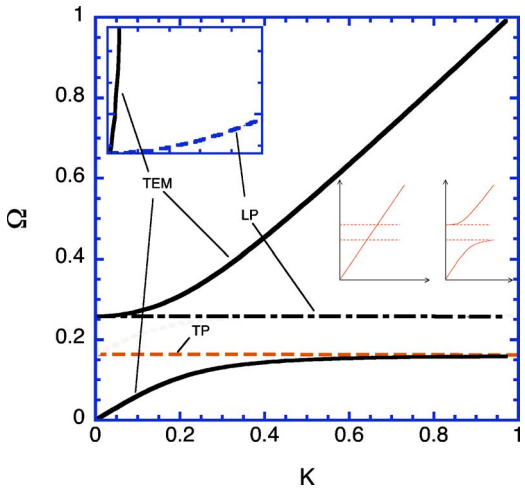

FIG. 2. (Color online) Band structure for the dipole crystal in the long wavelength limit, for $\Omega_0=\Omega_p=0.2$. Solid lines represent the TEM branches as given by Eq. (13). The upper dot-dashed line is for the LP, and the lower dashed for the TP mode. Inset in the upper-left corner shows a zoomed-in section of the dispersion diagram. The inset in the middle-right section shows a schematic of the band anti-crossing with TP and LP lines.

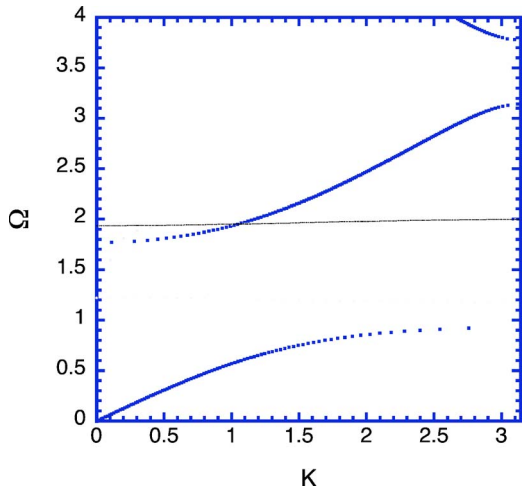

FIG. 3. (Color online) Band structure for $\Omega_0=\Omega_p=1.5$. The dotted line represents the TEM modes, and the thin line is the LP mode. $K=\pi$ represents the edge of the Brillouin zone.

branches are as follows. For $K\to\infty$ the upper branch yields the vacuum light line $\Omega=K$, and the lower branch $\Omega=\Omega_T(K)$. For $K\to 0$ the lower branch yields the light line in the effective medium with the dielectric constant $\varepsilon(0,0)$, i.e., $\Omega=K/\sqrt{\varepsilon(0,0)}$, and the upper $\Omega=\bar{\Omega}_L(K)=\Omega_L(K)$ [last equality from Eq. (10)]. Thus a gap opens, as sketched in the middle-right inset in Fig. 2, which can be viewed as a result of an avoided crossing of the vacuum photon mode with the polarization modes of the medium. The left panel in the inset shows schematically the vacuum light line and the two polarization modes *before*, and the right one *after* the interaction of photons with the dipolar polarization fields was "switched-on."

The general solution of Eq. (1), not restricted to the long wavelength limit, has a simple form for the cubic array

$$K=f(\Omega)=\arccos\left[\frac{B_1\pm\sqrt{B_1^2-8v(1)B_2}}{4v(1)}\right] \tag{15}$$

where

$$B_1=A+2v(1)\cos\Omega \tag{16}$$

$$B_2=A\cos\Omega+\tfrac{1}{2}\Omega\sin\Omega \tag{17}$$

$$A=\frac{\Omega^2-\Omega_0^2}{\Omega_p^2}-v(0) \tag{18}$$

Figure 3 shows the mode band structure in this case for large $\Omega_0=\Omega_p=1.5$. The dotted line represents the TEM modes, and the thin line is the LP mode. $K=\pi$ represents the edge of the Brillouin zone. Note the Umklapp of the TEM mode and the gap opening at this edge. Thus, this point dipole array is a *photonic band gap crystal*. The LP mode is seen to intersect with the TEM mode. This, however, does not imply the mode interaction, since *no avoided crossing* of the two modes occurs at the crossing point.

The LP can be excited by a *p*-polarized, incoming electromagnetic field at the crystal surface. In the long wavelength limit ($\Omega\ll 1$) the point-dipole crystal is expected to act as an effective medium, with a dielectric function *n* given by Eq. (5). Then, the reflection coefficient (at a normal incidence) from a surface of such an effective medium is

$$r=\frac{n-1}{n+1} \tag{19}$$

Mahan and Obermair[1] have calculated *r* exactly (directly from their formalism) in the long wavelength limit, and found that indeed it is essentially indistinguishable from Eq. (19). Using this excellent effective medium approach, we consider next a finite thickness slab of the point dipole crystal, placed in vacuum. The slab is parallel to the *x*-*y* plane, and extends from $z=-d$ to $z=0$. All fields are assumed to be $\propto\exp i(k_x x-\omega t)$. There are two transverse waves for $z<-d$ (in vacuum) with *z*-components electric field amplitudes $E_{0z}=1$ and E_{1z}, four waves inside the slab (two transverse E_{2z} and E_{4z}, and two longitudinal E_{3z} and E_{5z}), and only one (transverse) for $z>0$ (in vacuum) E_{6z}. By requiring that the total electric field, and the perpendicular to the surface of the slab current ($j_z=\sigma_\perp E_{z\perp}+\sigma_\parallel E_{z\parallel}$; where symbol $\perp$ represents transverse, and $\parallel$ longitudinal components) are continuous across both interfaces,[9] we obtain the following matrix equation for the *z*-components of the electric fields

$$\begin{bmatrix} s_1 & -1/s_2 & -1/p & -s_2 & -p & 0 \\ K_1 s_1 & K_2/s_2 & -\beta/p & -K_2 s_2 & \beta p & 0 \\ 0 & \alpha/s_2 & 1/p & \alpha s_2 & p & 0 \\ 0 & 1 & 1 & 1 & 1 & -1 \\ 0 & -K_2 & \beta & K_2 & -\beta & K_1 \\ 0 & \alpha & 1 & \alpha & 1 & 0 \end{bmatrix} \begin{bmatrix} E_{1z} \\ E_{2z} \\ E_{3z} \\ E_{4z} \\ E_{5z} \\ E_{6z} \end{bmatrix} = \begin{bmatrix} -1/s_1 \\ K_1/s_1 \\ 0 \\ 0 \\ 0 \\ 0 \end{bmatrix} \tag{20}$$

where $K_1=\Omega\cos\Theta$, $K_2=\sqrt{\Omega^2\varepsilon(\bar{\Omega})-K_x^2}$, and $K_x=\Omega\sin\Theta$. Θ is the angle of incidence for the incoming wave at $z=-d$. $\varepsilon(\bar{\Omega})$ is the dielectric function given by Eqs. (5) and (11), but for $K\to 0$, and with Ω^2 replaced by $\bar{\Omega}^2=\Omega(\Omega+i\Gamma)$, where Γ is the effective damping parameter. $s_i=\exp(iK_iD)$, where $i=1,2$, and $D=d/a$. $p=\exp(iL_2D)$, where $L_2=\sqrt{K_{\text{long}}^2-K_x^2}$. K_{long} is obtained by inverting Eq. (12), in which Ω^2 is replaced by $\bar{\Omega}^2$. $\alpha=\sigma_\perp/\sigma_\parallel=1-\varepsilon(\bar{\Omega})$, where the conductivities are defined through $\varepsilon(\bar{\Omega})=1+4\pi i\sigma_\perp/\Omega$, and $\varepsilon_\parallel=0=1+4\pi i\sigma_\parallel/\Omega$. Finally $\beta=K_x^2/L_2$. Equation (20) can be analytically solved for E_{6z}, yielding the transmission coefficient

$$t=E_{6z}=\frac{B_1}{s_1B_2} \tag{21}$$

where

$$B_1=4\varepsilon(\bar{\Omega})K_1[\alpha\beta(s_2-1/s_2)+K_2(p-1/p)] \tag{22}$$

$$\begin{aligned} B_2=&(1/s_2)(K_1+K_2)[(K_1+K_2)(1/p-p)+\alpha(K_1-\beta)\\ &\times(s_2-1/p)+\alpha(K_1+\beta)(p-s_2)]+s_2(K_1-K_2)\\ &\times[(K_1-K_2)(p-1/p)+\alpha(K_1-\beta)(1/p-1/s_2)\\ &+\alpha(K_1+\beta)(1/s_2-p)]-\alpha(1/p)(K_1-\beta)\\ &\times[(K_1+K_2)(1/s_2-p)+\alpha(K_1-\beta)(s_2-1/s_2)\\ &+(K_1-K_2)(p-s_2)]-\alpha p(K_1+\beta)\\ &\times[(K_1-K_2)(s_2-1/p)+(K_1+K_2)(1/p-1/s_2)\\ &+\alpha(K_1+\beta)(1/s_2-s_2)] \end{aligned} \tag{23}$$

Figure 4 shows plot of tt^* (transmittance) versus Ω for a slab of thickness $D=100$, and for $\Theta=0$. The dipole crystal has $\Omega_0=\Omega_p=0.05$. The transmittance calculated with the use of the full nonlocal formula [Eqs. (21)–(23)] is indistinguishable from that obtained from the local formula[10]

$$t_{loc}=\frac{4\varepsilon(\bar{\Omega})K_1K_2s_2(1/s_1)}{[\varepsilon(\bar{\Omega})K_1+K_2]^2-[\varepsilon(\bar{\Omega})K_1-K_2]^2s_2^2} \tag{24}$$

This is to be expected, since at normal incidence the longitudinal modes cannot be excited. tt^* is essentially zero in the gap, as expected. There are also peaks due to Fabry-Perot (FP) resonances of the transverse waves in the slab, at which $K_2D=s\pi$, where $s=1,2,3\ldots$.

To activate the longitudinal waves we increase the angle of incidence Θ. Figure 5 shows calculation for $\Theta=45$ deg, for a very thin slab with $D=10$. Now there is a difference between local and nonlocal results. First, the evanescent transmission in the gap region is slightly higher for the nonlocal case. Secondly, in addition to the FP resonances of the transverse waves, FP resonances of the longitudinal waves, multiply reflected between the surfaces of the slab, appear in the narrow band at $\Omega\approx 0.066$ (see the inset). While the above calculations are carried out with $\Gamma=0.0002$ ($Q\approx\Omega/2\Gamma\approx 165$), these resonances are still visible for slabs with damping constant $\Gamma=0.0005$ ($Q\approx 66$). Note, that propagation of these longitudinal waves is essentially perpendicular to the surface, since $L_2\gg K_x$ at this frequency.

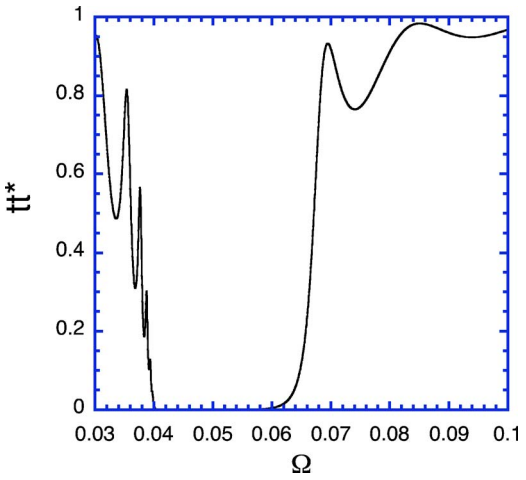

FIG. 4. (Color online) The transmittance tt^* vs frequency Ω for a slab of thickness $D=100$, and for $\Theta=0$.

The dielectric function (5) can be written in the Lyddane-Sachs-Teller form

$$\varepsilon(\Omega,K)=\frac{\bar{\Omega}_L^2(K)-\Omega^2}{\Omega_T^2(K)-\Omega^2} \tag{25}$$

In the long wavelength limit this reduces to

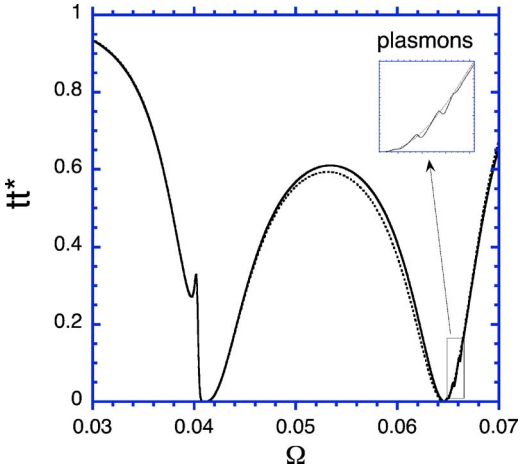

FIG. 5. (Color online) The transmittance tt^* vs frequency Ω for a slab of thickness $D=10$, and for $\Theta=45$ deg.

$$\varepsilon(\Omega,0)=\frac{\Omega_0^2+\frac{2}{3}\Omega_p^2-\Omega^2}{\Omega_0^2-\frac{1}{3}\Omega_p^2-\Omega^2} \tag{26}$$

from which we find that $\varepsilon(\Omega_S,0)=-1$ at the frequency $\Omega_S=\sqrt{\Omega_0^2+(1/6)\Omega_p^2}$. At this frequency there will exist surface plasmons localized at the crystal-vacuum interface. It has been shown by Pendry,[11] that at the surface plasmon frequency a very thin ($d\ll\lambda$) film of the material can amplify evanescent waves, and can thus act as a superlens. Our detailed calculation shows that a very thin film of a crystal made of Ag nanoparticles indeed superlenses, similarily to a thin Ag film,[11,12] but is less efficient. Details of this investigation will be given elsewhere.

Finally, we consider possibility of the negative refraction in the point-dipole crystal. This effect, originally proposed by Veselago,[13] occurs in media with $n=-1$. Since such a medium does not occur in nature, a practical way was proposed to fabricate them by using a network of wires and the so called split-ring resonators.[14] It has been shown, that a two-dimensional photonic crystal can also simulate such a medium,[15] and that the negative refraction can occur at the center of the Brilluoin (i.e., Γ-point) if the second photonic band has a negative curvature. This scenario can be achieved in the point-dipole crystal. To show this, we first modify the theory to allow for the crystal to be immersed in a dielectric background (with a dielectric constant ε_b). This can be accounted for by simply replacing (in all the above equations) Ω, Ω_0, and T, with $\Omega\sqrt{\varepsilon_b}$, $\Omega_0\sqrt{\varepsilon_b}$, and $T\varepsilon_b$, respectively. We consider a crystal with the following parameters: $\Omega_0=\Omega_p=3$, and $\varepsilon_b=5$ (e.g., TiO in the visible frequency range). Figure 6 below shows the corresponding dispersions. There are three TEM mode branches, with the middle, and the top one exhibiting strong negative slopes. The sketch in the inset in Fig. 6 clarifies the topology of the bands. It is the minimum-bending avoided-crossing of the photon line with the LP and TP asymptotics, as before, but this time the photon line is "Umklapped" at the Brilluoin zone, before crossing the asymptotics. The left panel in the inset shows the case before, and right panel after the mode interaction has been "switched on." While the top branch is entirely due to "Umklapp," the middle one has a strongly polaritonic nature. This branch has a negative slope (controlled by a choice of Ω_0 and Ω_p), and therefore the negative refraction is expected at the frequency given by the intersection of the vacuum light line with this branch. This negative refraction is mediated by polaritonic waves rather than by the pure TEM modes, which is usually the case in photonic crystals. Similar effects were observed recently in two-dimensional polaritonic crystals of metallic rods.[16–18]

We now discuss possible manufacturing scenarios for the point-dipole crystal. For tests in the microwave frequency range we propose a cubic crystal of small spheres made of BSTO($Ba_{1-x}Sr_xTiO_3$)-oxide composite ceramics.[19] This material has dielectric constant $\varepsilon'=646$ and the loss tangent $\varepsilon''/\varepsilon'=0.004$ at $f=2.139$ GHz ($\lambda=14$ cm), and this allows for sharp Mie resonances to develop inside small spheres. Using the Mie theory we have found the resonance frequency to be given by $2\pi R/\lambda=0.123$, where R is the sphere radius. Here this yields $R=0.27$ cm. The polarizability of a single sphere is then given approximately by Eq. (11) with $\Omega_0=2\pi a/\lambda$. The lattice constant of this crystal should be $a\approx 1$ cm. For tests at visible frequencies one might use metallic nanoparticle arrays (e.g., Au nanospheres or nanorods) in a transparent matrix. Such nanoparticles can exhibit Mie resonances with $Q>25$,[20] and these lead to the desired form of the particle polarizability. Clearly the low value of Q is a problem in this case, and therefore, many of the phenomena discussed in this paper might become invisible. Another possibility is to employ films of metal atoms (e.g., Cr) periodically distributed in a transparent matrix (e.g., Al_2O_3). Such atoms also have the desired form of the polarizability, and in addition $Q\approx 1000$ can be expected since such materials (with random distribution of atoms) are used as active media of lasers (e.g., ruby).[21]

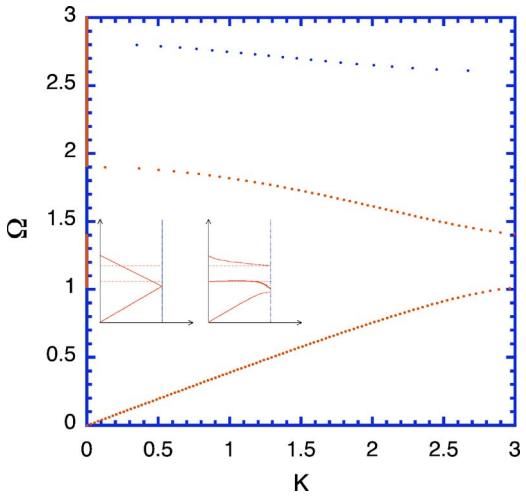

FIG. 6. (Color online) Band structure for $\Omega_0=\Omega_p=3$, and $\varepsilon_b=5$. The inset shows a schematic of the band anti-crossing with TP and LP lines.

In conclusion, we have studied the electromagnetic response of a cubic array of polarizable and resonant point dipoles. We show, that the system is a nonlocal polaritonic crystal, that allows for bulk and surface plasmon wave propagation in addition to the usual photonic crystal effects (bands, gaps, etc.). In addition, a negative refraction, and a subwavelength lensing can occur for properly chosen parameters of the system. An experimental demonstration of these effects is possible, both at microwave and optical frequencies.

*On leave from: Department of Physics, Boston College, Chestnut Hill, Massachusetts 02467, USA
†On leave from: Soreq NRC, Yavne 81800, Israel

[1] G. D. Mahan and G. Obermair, Phys. Rev. **183**, 834 (1969).
[2] P. Bakshi, D. A. Broido, and K. Kempa, Phys. Rev. B **42**, 7416 (1990).
[3] G. F. Giuliani and J. J. Quinn, Phys. Rev. Lett. **51**, 919 (1983); J. K. Jain and Ph. B. Allen, *ibid.* **54**, 2437 (1985).
[4] C. Yannouleas, E. N. Bogachek, and U. Landman, Phys. Rev. B **53**, 10225 (1996).
[5] K. Kempa, Phys. Rev. B **66**, 195406 (2002).
[6] See, for example, U. Kreibig, M. Vollmer, *Optical properties of metal clusters* (Springer, Berlin, 1995).
[7] J. D. Jackson, *Classical Electrodynamics* (Wiley, New York, 1975).
[8] They are retarded, in fact much stronger, by the material inertia of the charges involved.
[9] F. Forstmann and R. R. Gerhardts, Festkoerperprobleme **22**, 291 (1982).
[10] Z. Ye, Phys. Rev. B **67**, 193106 (2003).
[11] J. B. Pendry, Phys. Rev. Lett. **85**, 3966 (2000).
[12] R. Ruppin, J. Phys.: Condens. Matter **17**, 1803 (2005).
[13] V. G. Veselago, Sov. Phys. Usp. **10**, 509 (1968).
[14] D. F. Sievenpiper, M. E. Sickmiller, and E. Yablonovitch, Phys. Rev. Lett. **76**, 2480 (1996); J. B. Pendry, A. J. Holden, W. J. Stewart, and I. Youngs, *ibid.* **76**, 4773 (1996); J. B. Pendry, A. J. Holden, D. J. Robbins, and W. J. Stewart, J. Phys.: Condens. Matter **10**, 4785 (1998); J. B. Pendry, A. J. Holden, D. J. Robbins, and W. J. Stewart, IEEE Trans. Microwave Theory Tech. **47**, 2075 (1999).
[15] M. Notomi, Phys. Rev. B **62**, 10696 (2000); S. Foteinopoulou, E. N. Economou, and C. M. Soukoulis, Phys. Rev. Lett. **90**, 107402 (2003); E. Cubukcu, K. Aydin, E. Ozbay, S. Foteinopoulou, and C. M. Soukoulis, Nature (London) **423**, 604 (2003); X. Wang, Z. F. Ren, and K. Kempa, Opt. Express **12**, 2919 (2004).
[16] X. Wang and K. Kempa, Phys. Rev. B **71**, 233101 (2005).
[17] M. I. Antonoyiannakis and J. B. Pendry, Europhys. Lett. **40**, 613 (1997).
[18] M. I. Antonoyiannakis and J. B. Pendry, Phys. Rev. B **60**, 2363 (1999).
[19] S. O'Brien and J. B. Pendry, J. Phys.: Condens. Matter **14**, 4035 (2002).
[20] C. Sönnichsen, T. Franzl, T. Wilk, G. von Plessen, J. Feldmann, O. Wilson, and P. Mulvaney, Phys. Rev. Lett. **88**, 077402 (2002).
[21] T. M. Hensen, M. J.A. de Dood, and A. Polman, J. Appl. Phys. **88**, 5142 (2000).